



Explosions in closed pipes containing baffles and 90 degree bends

Robert Blanchard*, Detlef Arndt, Rainer Grätz, Marco Poli, Swen Scheider

BAM Federal Institute for Materials Research and Testing, Chemical Safety Engineering, Explosion Protection and Risk Assessment, Unter den Eichen 87, 12205 Berlin, Germany

ARTICLE INFO

Article history:

Received 11 May 2009

Received in revised form

3 September 2009

Accepted 3 September 2009

Keywords:

Explosion enhancement

Deflagration to detonation transition

Bend

Baffle

ABSTRACT

There is a general lack of information on the effects of full-bore obstacles on combustion in the literature, these obstacles are prevalent in many applications and knowledge of their effects on phenomena including burning rate, flame acceleration and DDT is important for the correct placing of explosion safety devices such as flame arresters and venting devices. In this work methane, propane, ethylene and hydrogen–air explosions were investigated in an 18 m long DN150 closed pipe with a 90 degree bend and various baffle obstacles placed at a short distance from the ignition source. After carrying out multiple experiments with the same configuration it was found that a relatively large variance existed in the measured flame speeds and overpressures, this was attributed to a stochastic element in how flames evolved and also how they caused and interacted with turbulence to produce flame acceleration. This led to several experiments being carried out for one configuration in order to obtain a meaningful average. It was shown that a 90 degree bend in a long tube had the ability to enhance flame speeds and overpressures, and shorten the run-up distance to DDT to a varying degree for a number of gases. In terms of the qualitative effects on these parameters they were comparable to baffle type obstacles with a blockage ratios of between 10 and 20%.

© 2009 Published by Elsevier Ltd.

1. Introduction

Explosions in the process industry are still a significant problem leading to injuries, death, destruction of equipment and downtime. As a consequence there is a need in many chemical processes for protection against propagation of unwanted combustion phenomena such as deflagrations and detonations (including decomposition flames) in process equipment, piping and vent manifold systems (vapour collection systems) (Grossel, 2002). Environmental and safety concerns relating to volatile organic solvents (VOCs) have also, in recent years, lead to a vast increase in the amount of piping and number of systems handling flammable fuel air mixtures for collection, containment and transport. Control over these mixtures is also required until flammable gases can be destroyed or safely discharged (Newsholm, 2004). In many of the above situations, in order to aid ATEX compliance, correctly placed and specified flame arresters are needed, dependent on the conditions they are likely to encounter. However, there is still some uncertainty over where best to locate these devices and concerns have been raised with safety standards for flame arrestors in regards to the lack of knowledge of where deflagration to denotation will/can occur in a pipe and what factors can contribute to this effect (Oakley & Thomas, 2004). These concerns

persist still to this day and as part of a safety concept related to flame arrestor positioning it is important to be able to predict the mode of burning at various points in a pipe.

Explosions in pipes and ducts, flame acceleration and the transition from deflagration to detonation are well researched subjects (Ciccarelli & Dorofeev, 2008). However, research in this area tends to concentrate on the effects of baffle type obstacles or items in the path of the flow (Ibrahim & Masri, 2001; Masri, Ibrahim, Nehzat, & Green, 2000). Tube bends, for example, are full-bore obstacles used extensively in industrial applications, however little is known about their effects on flame acceleration, overpressure enhancement and their contribution to DDT.

1.1. Research aim

The aim of the research presented in this paper is to communicate data from explosion experiments in an industrial-scale closed pipe containing a 90 degree bend in order to better understand and quantify the affects these types of obstacle can have on flame acceleration and DDT. Experimental data is also compared to that found using baffle type obstacles in the same position as the 90 degree bend.

1.2. Background

Fluid and particle flow through pipe bends is a well understood subject due to its associated practical problems in the process

* Corresponding author. Tel.: +49 30 8104 4258; fax: +49 30 8104 1217.
E-mail address: robblanchard@hotmail.com (R. Blanchard).

industry (Berger, Talbot, & Yao, 1983; Burgess, 1971; Green, 1999), however little research has been carried out on explosions through pipe bends, a complicated problem involving the interaction between fluid dynamics, heat transfer and (turbulent) combustion. In the first work carried out on this theme Phylaktou, Foley, and Andrews (1993) showed that with a short tube a 90 degree bend can enhance to both the flame speed and the overpressure for methane–air explosions compared to similar experiments carried out in straight pipes. The flame speed in these experiments was enhanced by a factor of approximately five and was equated to the effects of a baffle with a blockage ratio of 20% at the same position.

Sato, Sakai, and Chiga (1996) investigated the effects of ignition position on the shape of the flame front and the flame speed for methane–air explosions using an open ended small square channel containing a 90 degree bend. However, only a limited number of experiments were carried out and no comparison was given to an experimental set-up without the bend.

A 24% enhancement of the flame speed after a 90 degree bend placed half-way down a tube was observed in propane–air experiments by Chatrathi (1992), the pipe diameter used for these experiments was 152.4 mm and the pipe was open at the end furthest from the ignition source.

Observations of the flame front when travelling through a rectangular 90 degree bend were made by Zhou, Sobiesiak and Quan (2006), who showed that after initially propagating as a flat flame the flame front takes on the tulip configuration (Clanet & Searby, 1996; Gonzalez, Borghi, & Saouab, 1992). As the flame reached the bend the upper tongue (the one propagating towards the outside of the bend) of the tulip slowed down, relatively. Whereas the lower tongue the one propagating towards the inside of the bend began propagating more quickly around the inside of the bend, an effect named “flame shedding” by the authors. 3-D particle modelling of the flow around the bend showed that large vortices were created just downstream of the inside wall of the bend while flow followed a more streamlined pattern around the outside of the bend. This was in good agreement with latter constant temperature anemometry (CTA) observations made by Lohrer, Hahn, Arndt, and Grätz (2008) who showed that a bend induced a significant increase in turbulence over the first 30% of the inner diameter of the pipe immediately after the bend. Whereas, only a relatively small amount of turbulence was induced around the outer side. Unfortunately in the study of Zhou et al. the bend was relatively close to the end of the tube giving little opportunity to observe the effect of the bend on downstream flow patterns.

Explosions (propane–air) have also been carried out in coiled pipes and pipes with multiple U-shaped bends (Frolov, 2008), while these configurations were able to produce fast DDTs, they are generally of more interest for pulse detonation engines

(Roy, Frolov, Borisov, & Netzer, 2004), where fast DDT is a requirement, rather than for industrial-scale pipework carrying potentially flammable gas.

2. Experimental

2.1. Apparatus

A horizontal DN150 steel pipe, shown in Fig. 1, was used for the following tests ($d = 159$ mm). This pipe was made up of a number of segments ranging from 2 to 5 m in length, bolted together with a gasket seal in-between the connections and blind flanges at both ends. Evacuation prior to introduction of the test gas confirmed no significant leaks were present in the pipe. Early work employing constant temperature anemometry techniques (Lohrer, Drame, Schalaus, & Grätz, 2008) had also shown that these connections introduced no significant turbulence inducing element to flow along the pipe. The total length of the pipe was approximately 18 m (L), giving an L/d ratio of 112.

Several tests utilised a 90 degree bend segment, this bend had a radius of 0.285 m and added a further 0.447 m to the length of the pipe (based to the centreline length of the segment). Initially this 90 degree segment was placed at a distance of 2 m from the ignition source. Due to the constraints of the dimensions of the room where tests were carried out this was the maximum allowable distance before the pipe bend. Several tests also utilised baffles, these were made from 3 mm thick sheet metal and were placed in-between connections in the pipe. Baffles used in these tests had sharp 90 degree corners and were made in 10% blockage ratio increments. The blockage ratio is defined as the surface area of the obstacle in the pipe over the cross sectional area of the pipe.

2.2. Sensors and data collection

The pipe contained sensor penetrations every 0.5 m in the axial direction which were used to position photodiodes and pressure transducers. Penetrations not used were filled with plugs which sat flush with the inside of the tube.

The position, and hence the speed, of the flame front was determined using BPY 62 Silicon NPN phototransistors (OSRAM) placed at metre intervals along the entire length of the pipe.

The pressure at various points along the length of the pipe was recorded using piezoelectric pressure transducers (PCB M113A22, 1.5 ± 0.005 mV/kPa) with the signal being processed by a PCB 481 Sensor Signal Conditioner. Pressures reported are the absolute maximum side-on overpressures recorded during experiments and the maximum side-on overpressures after a smoothing function had been applied to original pressure-time signals.

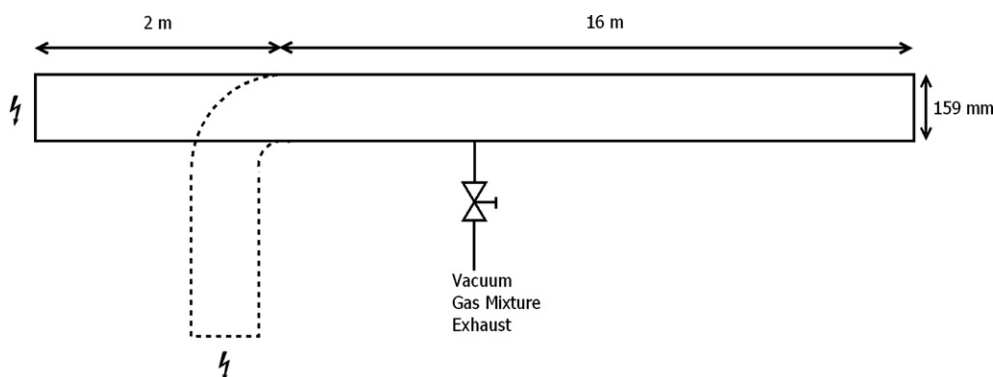


Fig. 1. Schematic of the pipe used for explosion experiments.

All sensors were flush with the inside surface of the tube in order to avoid any additional turbulence enhancement. Data from all sensors was collected at a frequency of 0.18 MHz.

2.3. Gas mixtures

Gas mixtures were produced using the partial pressure method and mixed by a paddle in a rocking tube. After sufficient time the gas mixture was introduced to the evacuated pipe, to the desired pressure. All gas mixtures used during these experiments were at stoichiometric concentration and ambient pressure, unless otherwise stated. The gases used for the following experiments were methane, propane, ethylene and hydrogen.

Gas mixtures were ignited at one end of the pipe using a melting wire (ignition energy approximately 10 J). The position of the ignition source has a significant effect over the initial propagation of the flame and the resulting flame speeds and overpressures (Phylaktou & Andrews, 1991a, 1991b), so was kept at a constant position flush at the centre of one of the blind flanges. Ignition was detected using a phototransistor placed close to the ignition source, this phototransistor also triggered the data logging system.

For most experimental configurations a number of tests (minimum three) were carried out depending on the reproducibility of the flame speeds and overpressures.

3. Results and discussion

3.1. Methane experiments

Experiments were first carried out with methane–air mixtures in a straight pipe. These initial experiments were then compared to a series of methane–air explosions carried out utilising the 90 degree bend and baffle obstacles detailed in the previous section. The first striking observation was the variability of flame speeds and overpressures measured during experiments using the same apparatus, test gas mixture and method.

The maximum flame speed along the length of the pipe for six methane–air explosions varied from approximately 20–80 ms^{-1} , many of these explosions also showed two relatively large peaks in

the flame speed between 30 and 60% of the pipe length (all flame speed data for these and other experiments discussed in this paper can be found online at <http://www.XXXlink> to Elsevier websiteXXX). It is difficult to determine the exact cause for the variance in these resulting flame speeds as there are complicated interactions involved, and a stochastic element in how the flame evolves and then causes and interacts with turbulence to produce flame acceleration. All pre-set variables were controlled within the confines of experimental error. However, possible sources of this variance could have derived from the exact nature of the ignition event, localised wall characteristics and small changes in the gas consistency etc. This phenomena should be further investigated as it could have significant consequences for the standard testing of items such as flame arresters (European Standard EN 12874, 2001) where, for example, a pre-set number of deflagrations should be unable to pass through an arrester element in order for it to be certified. These tests are assumed to be on the conservative-side due to the tube being closed at both ends. However, if explosions were all at the lower end of the spectrum in terms of flame speeds and overpressures then the flame arrester may not be able to withstand harsher conditions produced by the same gas mixture in similar equipment at another time. The oscillations seen in the flame speed are a common occurrence during these types of explosion and are attributed to complicated interactions between flame acceleration, quenching on the walls of the pipe, changes in the shape of the flame front (Phylaktou & Andrews, 1991a, 1991b) and interactions with pressure waves reflected by the closed end of the pipe. The pressure measured at a number of points along the length of the pipe was seen to be relatively similar regardless of the measurement position. For these “slow deflagration” experiments this was due to the pressure waves caused by the explosion travelling considerably faster than the flame front, meaning that a pressure sensor in these experiments saw approximately the same pressure profile wherever it was placed in the pipe.

Examples of flame speeds for methane–air explosions in four pipe configurations; straight, and with a 10, 20 and 30% BR baffle are shown in Fig. 2, the vertical line in the graph represents the position of the obstacle. It should be noted that, in this Figure only one example of each experimental configuration is displayed in order to

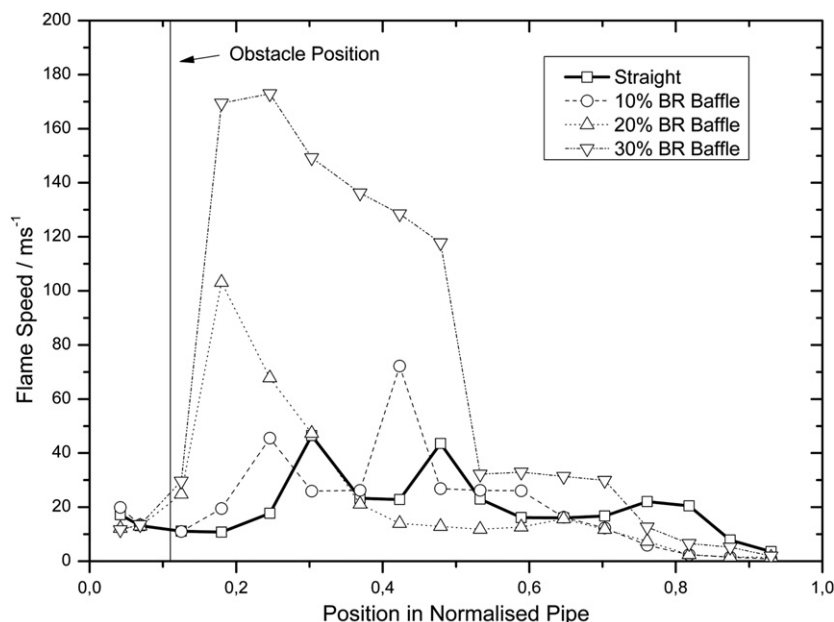


Fig. 2. Flame speeds for methane–air explosions with a 10, 20 and 30% BR baffle.

illustrate an effect. Also, in the following discussion flame speeds for these and other explosions are always compared to those found in the straight configuration, which is taken to be the base case.

The use of all three baffles resulted in higher downstream flame speeds being recorded as the blockage ratio of the baffles increased. This effect has been observed by many research groups and is widely accepted to be due to turbulence inducing elements enhancing the heat and mass transfer in reactive flows (Andrews, Herath, & Phylaktou, 1990; Phylaktou & Andrews, 1991a, 1991b; Starke & Roth, 1989).

No large difference in the initial flame speeds for the straight configuration and the configuration with the 10% BR baffle were seen, indicating that the 10% BR baffle has little effect on upstream flow. The 20 and 30% BR baffles induced some flame acceleration before the baffle possibly due to flow contraction. However, the majority took place behind the obstacle. Interestingly, the 10% baffle configuration shows some acceleration after the obstacle but the maximum flame speed is recorded further down the pipe after the flame had returned to similar speeds to that seen in the straight pipe configuration. Conventional wisdom would suggest that the accelerating effect of the baffle should be seen directly downstream of the obstacle. Therefore, to better explain these effects more sophisticated measurement techniques, visualisation of the flame and CFD would be needed.

The effect of a 90 degree bend on methane–air explosions at the same position as the aforementioned baffles was also compared. Examples of flame speeds produced using this, the straight and 10% BR baffle configurations are shown in Fig. 3. The bend configuration displayed slightly higher flame speeds upstream of the obstacle position than the straight and 10% BR baffle configurations. Both obstacles produced similar maximum flame speeds (approximately 70 ms^{-1}), however, the maximum flame speed seen during the explosion in the bend configuration occurred immediately after the obstacle, as would be expected from the accepted theory of flame acceleration by an obstacle. For the baffle configuration a smaller acceleration occurred immediately after the obstacle followed by a deceleration before a final acceleration during which the maximum flame speed was recorded. It is acknowledged that the form of the flame front will be different as it approaches and passes these obstacles, and therefore there will be differences in the way which the flame interacts with the turbulence caused by the obstacle, making a true quantitative comparison between the two is very difficult. However, knowledge of the qualitative effects of

these obstacles can be important in predicting flame acceleration phenomena in pipes.

The methane explosions are displayed in terms of their maximum flame speeds, overpressures (smoothed and peak) and maximum rates of pressure rise in Table 1. The maximum smoothed overpressure is the maximum recorded pressure after a smoothing function had been applied to the pressure–time history, whereas the maximum peak overpressure was the actual highest overpressure recorded by the sensor with no smoothing function applied.

Although there is some scatter, general trends in maximum flame speed can be seen from these experiments. Firstly there was no large difference in the maximum flame speeds for methane–air explosions when comparing the straight and bend configurations, indicating that the bend in this position induces only a relatively small amount of turbulence with which the flame can interact and accelerate. However, the maximum flame speed for the bend configuration was generally found at around 20% of the pipe length, directly after the obstacle position ($\sim 10\%$), whereas the maximum flame speeds for the straight configuration was found between 30 and 50% of the pipe length. This would indicate that, as with the 20 and 30% BR baffle configurations, the turbulence induced by the bend is significant and does cause an initial acceleration of the flame. Further downstream, may be due to quenching on the walls of the pipe or changes in the flame front geometry, the flame speed decelerated to speeds below those recorded in the straight pipe configuration between 30 and 50% of the pipe length.

The maximum flame speeds for 10% baffle configuration were also seen between 30 and 50% of the length of the pipe, and were on average higher than those produced in the straight pipe configuration. This suggests that while the baffle produced no immediate effect of increasing the rate of burning directly behind the obstacle it contributed to whatever effects were acting to accelerate the flame speed later on in the straight pipe configuration. As understanding the exact nature of these effects would require the quantification of complicated interactions between several factors (fluid dynamics, heat transfer and (turbulent) combustion), it is beyond the scope of this work and would require visualisation of the flame and more sophisticated measurement techniques. However, these results provide extremely useful information with regard to flame arrester placement and determining likely modes and rates of burning in a given system.

Maximum overpressures, both smoothed and peak, and the rate of pressure rise for each of these experimental configurations showed a large variation. For example, the maximum smoothed overpressure for experiments with the straight pipe configuration were recorded between 1 and 1.8 bar. This variance is again an important factor to take into account when determining how many explosions should be conducted during a standard test procedure.

Representative pressure vs. time profiles for the various configurations are shown in Fig. 4. The rate of pressure rise seen in these plots supports observations made concerning flame speeds. The straight, bend and 10% BR baffle configurations displayed relatively

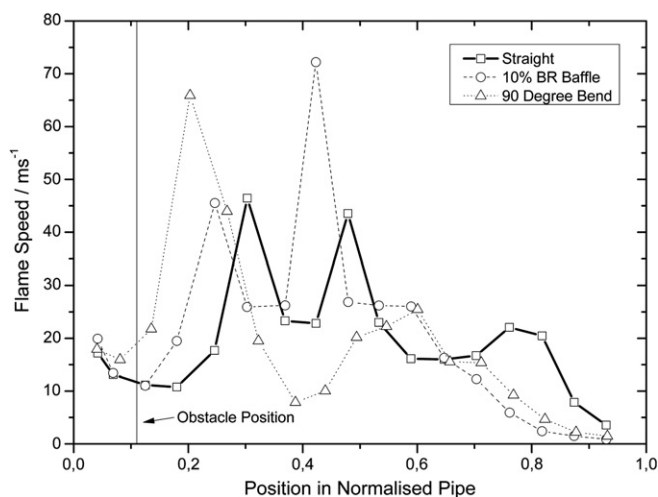


Fig. 3. Flame speed for methane–air explosions in straight, 10% BR baffle and 90 degree bend configurations.

Table 1

Flame speed and overpressure characteristics of methane explosions.

Configuration	Max. flame speed/ ms^{-1}		Max. overpressure (Smoothed)/bar		Max. overpressure (Peak)/bar		Max. rate of pressure rise/ bar s^{-1}	
	Average	SD	Average	SD	Average	SD	Average	SD
Straight	48.1	17.2	1.5	0.2	2.0	0.3	4.2	1.0
Bend	51.1	8.9	1.5	0.2	2.1	0.4	4.6	1.5
10% BR Baffle	82.2	20.9	1.4	0.2	2.4	0.5	5.0	2.5
20% BR Baffle	100.3	2.6	1.0	0.2	1.4	0.3	6.0	0.3
30% BR Baffle	149.8	20.3	1.1	0.1	1.6	0.3	6.8	1.6

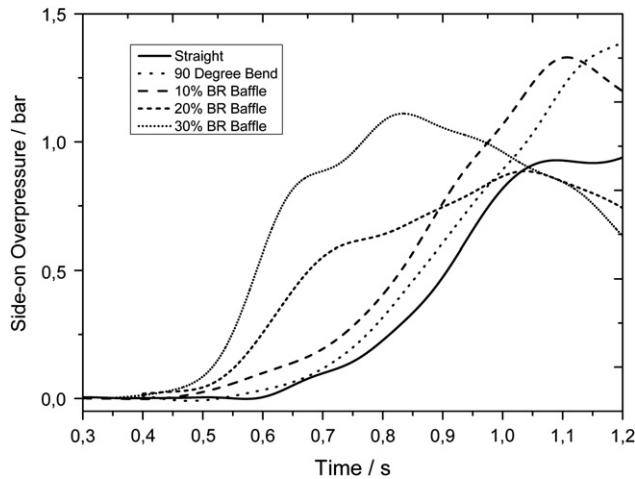


Fig. 4. Overpressure vs. time for methane-air explosions in straight, 10, 20, 30% BR baffle and 90 degree bend configurations.

similar flame speeds and rates of pressure rise, while the 20 and 30% baffle configurations showed higher rates of pressure rise which were associated with the observed higher burning speeds.

3.2. Propane experiments

Fig. 5 shows representative results from propane-air explosions utilising the straight pipe configuration and configurations with a 90 degree bend and a 20% BR baffle at 2 m from the ignition source.

Experiments carried out by Phylaktou et al. (1993) showed similar effects on the maximum flame speed when using a 90 degree bend or a 20% BR baffle. In their experiments the flame speed was enhanced by a factor of up to 6 times depending on the obstacle position. An enhancement factor of 2 was observed during these experiments which was due to the bend being placed closer to the ignition position giving the flame less time to accelerate before the obstacle and hence produce less turbulence downstream of the bend. In the experiments carried out by Phylaktou et al. it was assumed that the position which gave the maximum flame speeds for the baffle obstacle would also give the maximum flame speeds when using the bend. This may not always be the case, therefore, further experiments using different bend positions need to be carried out, however, unfortunately due to the dimensions of the test chamber this was not possible at present.

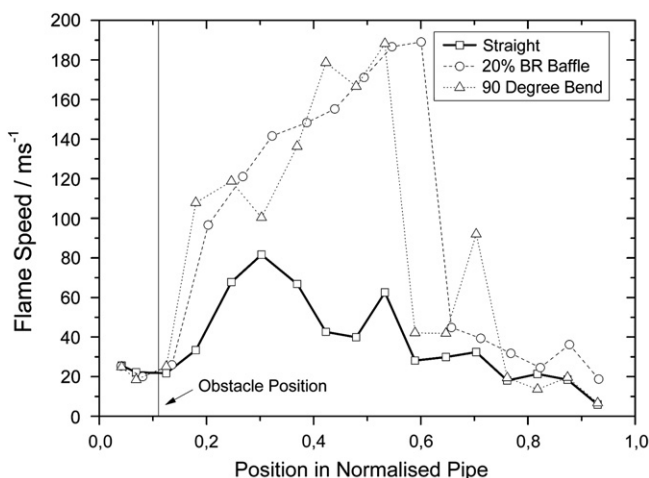


Fig. 5. Flame speeds for propane-air explosions.

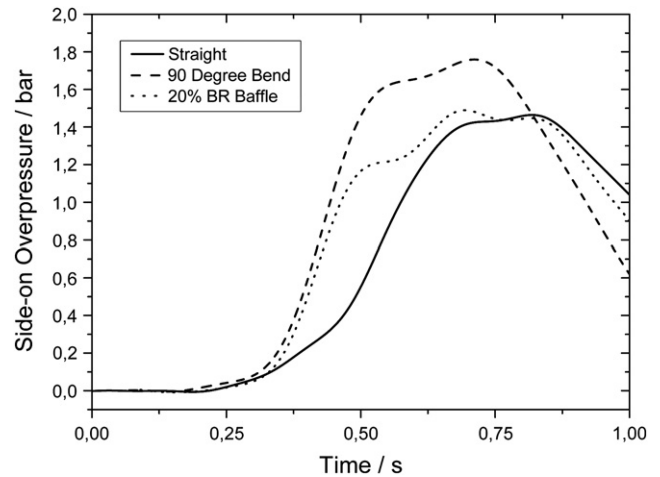


Fig. 6. Overpressure vs. time for propane-air explosions in straight, 20% BR baffle and 90 degree bend configurations.

Pressure vs. time records for propane experiments are shown in Fig. 6, from these it can also be seen that the burning rate was enhanced by an equal amount for both the bend and baffle configurations.

The average maximum flame speeds recorded during propane-air explosions are presented in Table 2 along with data on the maximum overpressures and maximum rates of pressure rise. While there is some spread in the results generally speaking the flame speeds produced using the bend and 20% BR configurations lay within the same range, reinforcing the hypothesis that a 20% BR baffle enhances the burning rate to the same degree as a 90 degree bend.

The maximum overpressures and rates of pressure rise produced during the experiments utilising the baffle and bend showed slightly higher values compared to the straight configuration, this may be expected due to the higher flame speeds recorded during these experiments but there is too much spread in the data to draw any firm conclusions.

One suspected DDT event was observed during the propane-air explosions using a baffle with a blockage ratio 30% (shown in Appendix A 2.4), during this experiment flame speeds reached close to 1000 ms⁻¹ and rates of pressure rise characteristic of detonative burning were observed.

3.3. Ethylene experiments

Flame speeds recorded during selected ethylene-air explosion experiments are shown in Fig. 7. Although flame speeds never reached the predicted C-J detonation velocity of 1822 ms⁻¹, it was believed that detonative or detonative-like combustion took place as pressure-time traces displayed the classic shape associated with detonative combustion and rates of pressure rise of several

Table 2

Flame speed and overpressure characteristics of propane explosions.

Configuration	Max. flame speed/ms ⁻¹		Max. overpressure (Smoothed)/bar		Max. overpressure (Peak)/bar		Max. rate of pressure rise/bar s ⁻¹	
	Average	SD	Average	SD	Average	SD	Average	SD
Straight	72.3	13.1	1.7	0.6	2.2	1.1	5.9	1.6
Bend	131.5	44.7	2.0	0.5	2.9	0.9	8.8	4.4
20% BR Baffle	133.1	43.9	1.8	0.2	2.5	0.4	7.1	2.1

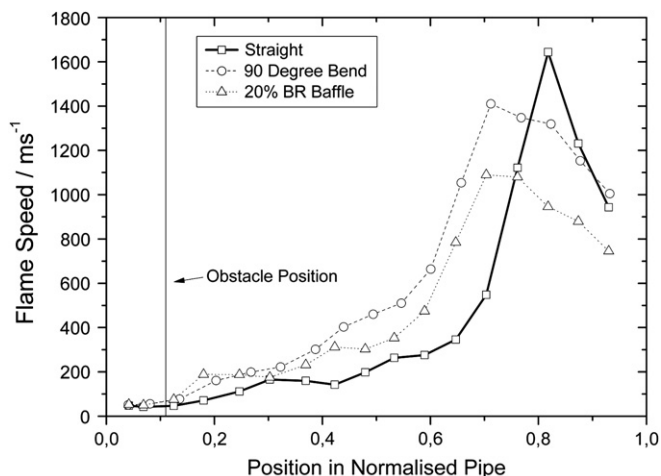


Fig. 7. Flame speeds for ethylene–air explosions.

thousand (bar s^{-1}) were observed. After the DDT (at between 70 and 80% of the pipe length) flame speeds decreased during the transition from overdriven detonation to stable-detonation. Interactions with reflected pressure waves from the closed end of the pipe may also have acted to slow the flame/pressure front. The maximum flame speed for the straight pipe configuration was observed at approximately 80% of the pipe length, whereas for the two configurations containing obstacles this maximum was at approximately 70%. On closer inspection of the flame speed profiles it can be seen that at approximately 20% of the pipe length (the obstacle is positioned at approximately 10% of the pipe length) the two obstacle containing configurations produced higher flame speeds than the straight configuration. While these flames decelerated slightly and returned to speeds closer to those which were observed in the straight configuration (at around 30% of the pipe length) they remained faster and therefore, assuming the maximum flame speed was associated with an overdriven detonation, DDT occurred over a shorter distance.

3.4. Hydrogen experiments

Flame speeds measured during three hydrogen–air explosions using the aforementioned pipe configurations are shown in Fig. 8. Each configuration used during these experiments produced

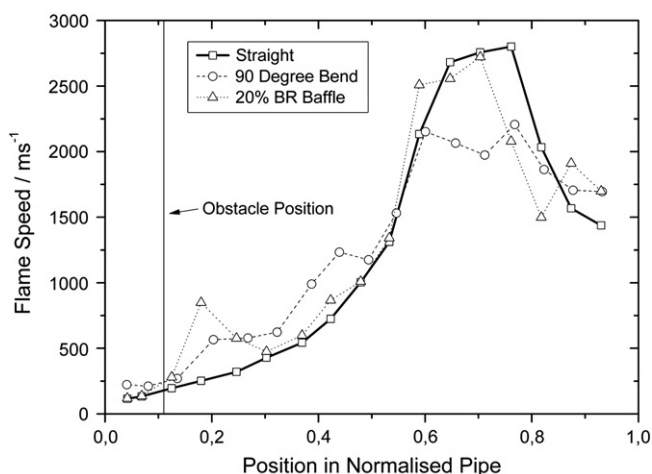


Fig. 8. Flame speeds for hydrogen–air explosions.

Table 3

Run-up distances to DDT for hydrogen–air explosions.

Configuration	Run-up distance to DDT	
	Average	SD
Straight	12.1	0.7
Bend	11.8	0.4
20% BR Baffle	10.9	0.5

a transition from deflagration to detonation. Interpretation of the flame speed data showed that the point at which the transition from fast deflagration to detonation occurred was between 60 and 80% of the pipe length, corresponding to between 68 and 96 pipe diameters. This transition was characterised by flame speeds over the CJ detonation velocity (1968 ms^{-1}) which typically occur during DDT and was confirmed by analysis of the form of pressure–time signals.

Both the baffle and the bend had an initial effect on the flame speed giving an acceleration after the obstacle. The largest increase in the flame speed, compared to the straight configuration, was observed with the 20% BR baffle where speeds of approximately 800 ms^{-1} are observed immediately downstream of the obstacle. The flame did not immediately transition into a detonation at this point, instead it returned to speeds similar to those seen in the straight pipe experiment before the transition into a detonation occurred further down the pipe (at approximately 60% of the pipe length). The same effects were observed for the 90 degree bend, however, the initial acceleration downstream of the obstacle was not as pronounced.

The run-up distance to DDT can be determined by analysis of shock waves from the overdriven detonation (Li, Lai, Chung, & Lu, 2005). A similar analysis was carried out for all hydrogen–air explosions, however, it was not possible for all ethylene and propane DDTs as the detonation shock waves from overdriven detonations were not strong enough to enable confident measurement of its velocity. The run-up distances to detonation for the hydrogen–air explosions described in this section are shown in Table 3. While the bend and baffle configurations showed similar flame speed profiles the baffle configuration was able to affect DDT over a shorter distance than the bend configuration. However, both bend and baffle configurations affected DDT over a shorter distance than the straight pipe configuration.

The flame acceleration caused by the obstacles was due to increases in downstream turbulence leading to faster burning and a faster transition to detonation, however, at approximately 30% and 50% of the length of the pipe, for the baffle and bend obstacles respectively, the flame speeds returned to those seen with the straight pipe configuration, these flames were then able to accelerate at rates faster than flames in the straight pipe configuration to undergo DDT over a shorter distance. This could be due to effects caused further downstream in the pipe after the initial acceleration or due to changes in the flame front shape at different points in the pipe. However in order to verify this hypothesis techniques such as high speed Schlieren or shadow photography would need to be employed in order to better position and visualise the flame.

4. Conclusions

These experiments showed for the first time the ability of a full-bore obstacle to accelerate the burning velocity of a number of gases and reduce the run-up distance required for DDT.

It was shown that a 90 degree bend placed at a relatively short distance from the ignition point in a long tube had the ability to enhance flame speeds and overpressures, and shorten the run-up distance to DDT. In terms of the qualitative effects on these parameters they were comparable to a baffle type obstacle with a blockage ratio of between 10 and 20%. It is expected that the flame speed enhancement caused by the 90 degree bend will be greater when the

obstacle is placed further downstream of the ignition point, due to the incoming flame having longer to accelerate and hence create a greater amount of turbulence downstream of the bend.

This work has contributed further to the argument that bends in a pipework system can have a significant effect on the combustion process, should be taken into account as part of a safety analysis and considered when placing explosion protection devices such as flame arresters or venting devices. Although this work has shown some interesting effects there are still many questions unanswered regarding the effects of obstacle position, multiple bends and other full-bore obstacles.

Interesting observations were also made on the variation of burning rates when using the same pre-set variables, an effect which needs to be further studied in order to determine the exact nature of the interactions which can contribute to flame acceleration.

Appendix. Supplementary information

Supplementary data associated with this article can be found, in the online version, at [doi:10.1016/j.jlp.2009.09.004](https://doi.org/10.1016/j.jlp.2009.09.004)

References

- Andrews, G. E., Herath, P., & Phylaktou, H. N. (1990). The influence of flow blockage on the rate of pressure rise in large L/D cylindrical closed vessel explosions. *Journal of Loss Prevention in the Process Industries*, 3(3), 291–302.
- Berger, S. A., Talbot, L., & Yao, L. S. (1983). Flow in curved pipes. *Annual Review of Fluid Mechanics*, 15, 461–512.
- Burgess, M. J. (1971). *Pressure losses in ducted flows*. London: Butterworth.
- Chatrathi, K. (1992). Deflagration protection of pipes. *Plant/Operations Progress*, 11(2), 116–120.
- Ciccarelli, G., & Dorofeev, S. (2008). Flame acceleration and transition to detonation in ducts. *Progress in Energy and Combustion Science*, 34(4), 499–550.
- Clanet, C., & Searby, G. (1996). On the 'tulip flame' phenomenon. *Combustion and Flame*, 105(1–2), 225–238.
- European Standard EN 12874. (2001). Flame arresters – Performance requirements, test methods and limits for use.
- Frolov, S. M. (2008). Fast deflagration-to-detonation transition. *Russian Journal of Physical Chemistry B*, 2(3), 442–455.
- Gonzalez, M., Borghi, R., & Saouab, A. (1992). Interaction of a flame front with its self-generated flow in an enclosure – the tulip flame phenomenon. *Combustion and Flame*, 88(2), 201–220.
- Green, D. W. (1999). *Perry's chemical engineers' handbook*. New York: McGraw-Hill.
- Grossel, S. S. (2002). *Deflagration and detonation flame arresters*. New York: American Institute of Chemical Engineers.
- Ibrahim, S. S., & Masri, A. R. (2001). The effects of obstructions on overpressure resulting from premixed flame deflagration. *Journal of Loss Prevention in the Process Industries*, 14(3), 213–221.
- Li, J., Lai, W. H., Chung, K., & Lu, R. K. (2005). Uncertainty analysis of deflagration-to-detonation run-up distance. *Shock Waves*, 14(5–6), 413–420.
- Lohrer, C., Drame, C., Schalaus, B., & Grätz, R. (2008). Propane/air deflagrations and CTA measurements of turbulence inducing elements in closed pipes. *Journal of Loss Prevention in the Process Industries*, 21(1), 1–10.
- Lohrer, C., Hahn, M., Arndt, D., & Grätz, R. (2008). Einfluss eines 90°-Rohrbogens in einer technischen Rohrleitung auf reaktive Strömungen. (in German). *Chemie Ingenieur Technik*, 80(5), 649–657.
- Masri, A. R., Ibrahim, S. S., Nehzat, N., & Green, A. R. (2000). Experimental study of premixed flame propagation over various solid obstructions. *Experimental Thermal and Fluid Science*, 21(1–3), 109–116.
- Newsholm, G. (2004). *Safe design and use of vent collection systems for potentially flammable mixtures*. HSE Online.
- Oakley, G. I., & Thomas, G. O. (2004). Investigations into concerns about BS EN 12874:2001 flame arresters. Performance requirements, tests methods and limits for use. HSE Research Report 281.
- Phylaktou, H., & Andrews, G. E. (1991a). Gas explosions in long closed vessels. *Combustion Science and Technology*, 77(1–3), 27–39.
- Phylaktou, H., & Andrews, G. E. (1991b). The acceleration of flame propagation in a tube by an obstacle. *Combustion and Flame*, 85(3–4), 363–379.
- Phylaktou, H., Foley, M., & Andrews, G. E. (1993). Explosion enhancement through a 90-degree curved bend. *Journal of Loss Prevention in the Process Industries*, 6(1), 21–29.
- Roy, G. D., Frolov, S. M., Borisov, A. A., & Netzer, D. W. (2004). Pulse detonation propulsion: challenges, current status, and future perspective. *Progress in Energy and Combustion Science*, 30(6), 545–672.
- Sato, K., Sakai, Y., & Chiga, M. (1996). Flame propagation along 90° bend in an open duct. In *Twenty-sixth symposium on combustion* (pp. 931–937). The Combustion Institute.
- Starke, R., & Roth, P. (1989). An experimental investigation of flame behavior during explosions in cylindrical enclosures with obstacles. *Combustion and Flame*, 75(2), 111–121.
- Zhou, B., Sobiesiak, A., & Quan, P. (2006). Flame behavior and flame-induced flow in a closed rectangular duct with a 90 degrees bend. *International Journal of Thermal Sciences*, 45(5), 457–474.

Nomenclature

- BR: Blockage ratio
 CTA: Constant temperature anemometry
 DDT: Detonation to deflagration transition
 SD: Standard deviation
 VOC: Volatile organic solvent